10.2478/v10160-012-0019-1

Transactions of the VŠB – Technical University of Ostrava

No. 2, 2012, Vol. XII, Civil Engineering Series

paper #15

Anežka JURČÍKOVÁ[1], Miroslav ROSMANIT[2]

THE POSSIBILITY OF USING NUMERICAL MODELING FOR ASSESSMENT OF WELDED JOINT LOAD-BEARING CAPACITY

MOŽNOST VYUŽITÍ NUMERICKÉHO MODELOVÁNÍ PRO POSOUZENÍ ÚNOSNOSTI SVAŘOVANÉHO STYČNÍKU

Abstract

The subject of this paper the practical example of the steel lattice structure was used. Specifically, the joint consisting of H-profile bottom chord and a RHS (Rectangular Hollow Section) brace members has been elected. This particular joint has an exceptional feature which is a deviation from the geometric conditions required by Eurocode. The aim is to create a numerical model that will adequately reflect the actual behavior of this type of joint as well as comparison of such behavior with that expected on the basis of assessment according to standardized formulas.

Keywords

Lattice structure, N-joint, FEM, RHS, H-profile.

Abstrakt

Jako námět této práce byl použit příklad ocelové příhradové konstrukce z praxe. Konkrétně byl zvolen styčník dolního pásu z HEA profilu a RHS mezipásových prutů, který je výjimečný tím, že se odchyluje od geometrických podmínek udávaných Eurokódem. Cílem práce je vytvoření numerického modelu, který bude dostatečně vystihovat skutečné chování takového styčníku a následné porovnání tohoto chování s tím, které je možné očekávat na základě posouzení dle normových vztahů.

Klíčová slova

Příhradová konstrukce, N-styčník, MKP, RHS, HEA.

1 INTRODUCTION

Nowadays, steel lattice structures consisting of hollow sections, or combinations of hollow sections and hot-rolled open sections, are often used on many structures. Such structures are suitable for overcoming large spans and their utilization has many advantages (biaxial cross section symmetry, shortened effective lengths, achievement of the required load-bearing capacity while preserving lightweight structure). On the other hand, design of joints may be problematic. Design methods given by Eurocode [1], are complicated, difficult to check, and offer a limited scope of use (geometric conditions, restrictions on material characteristics, certain types of joints of given types of loads).

[1] Ing. Anežka Jurčíková, Department of Structural Mechanics, Faculty of Civil Engineering, VSB-Technical University of Ostrava, Ludvika Podeste 1875/17, 708 33 Ostrava, tel.: (+420) 597 321 391, e-mail: anezka.jurcikova@vsb.cz.

[2] Ing. Miroslav Rosmanit, Ph.D., Department of Building Structures, Faculty of Civil Engineering , VSB-Technical University of Ostrava, Ludvika Podeste 1875/17, 708 33 Ostrava, tel.: (+420) 597 321 398, e-mail: miroslav.rosmanit@vsb.cz.

Therefore, the need increasingly arises to describe behaviour of joints beyond the scope of Eurocode limitations, for which standardized formulas for calculations of joints' load-bearing capacity cannot be applied exactly. For this paper we have selected a practical example – roofing with steel lattice girder containing H-profile chords and RHS web braces. This structure utilizes a joint outside of the Eurocode limitations for the use of the basic formulas in calculating the joint's load-bearing capacity. In particular, the angle of the tension brace connection to the bottom chord is smaller than 30°.

The aim of this work was to evaluate if the behaviour of such a joint, which does not fit the conditions of the standard, in spite of that could be described using established standardized procedures.

2 EXPECTED TYPES OF JOINT FAILURE ACCORDING TO EN 1993-1-8

The cited Eurocode [1] considers the following failure types for joints consisting of CHS (Circular Hollow Section) or RHS (Rectangular Hollow Section) web braces with I or H-profile cross section chords (cf. Fig. 1), see also [2] or [3]:

- **Failure of web plate** by plasticization, crushing or loss of shape stability;
- **Chord shear failure**;
- **Brace failure** (cracking in the welds or in the brace members).

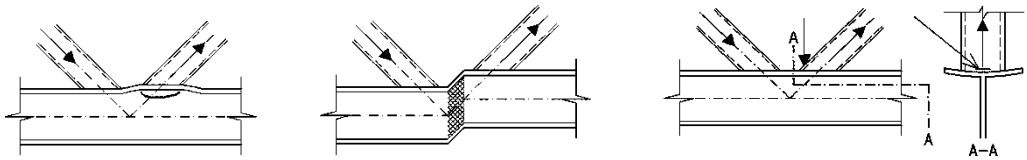

(a) (b) (c)

Fig. 1: (a) Failure of web plate; (b) Chord shear failure; (c) Brace failure

In formulas for calculation of the load-bearing capacity, with respect to different types of failures, the Eurocode does not take into account forces or tensions occurring in individual bars. It only considers the joint's geometry, profile types and values of the used materials' yield stresses. That is why the two different design setups were solved to compare behaviour of a joint loaded with force in the tension brace only, with that loaded with realistic forces (that is, both the force in the tension brace and tensile force in the bottom chord).

3 ASSESMENT OF THE SOLVED N-JOINT USING STANDARDIZED FORMULAS

Two design setups were considered for the joint investigated in this paper – first with a stiffener under the compression vertical brace only and the other with added stiffener under the tension diagonal brace. Geometry of the joint and the location of stiffeners are shown in Fig. 2.

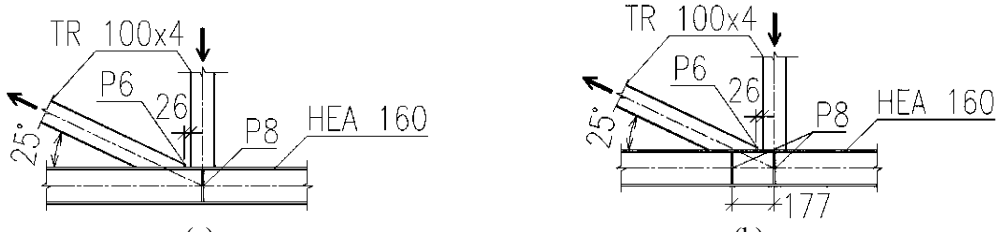

(a) (b)

Fig. 2: Geometry of the N-joint consisting of an H-profile chord and RHS web braces
(a) First design setup; (b) Second design setup

Although the joint does not satisfy one of the geometric conditions listed in the standard, an approximate assessment on the basis of standardized formulas was made for the both design setups. The load bearing capacity was calculated for the tension brace.

3.1 EN 1993 design procedure

1. Failure of web plate – buckling of the plate

$$N_{1,Rd} = \frac{f_{y0} \cdot t_w \cdot b_w}{\sin\theta_1} / \gamma_{M5} \tag{1}$$

where:

f_{y0} – yield stress of the bottom chord material [MPa],

h_1 – height of the brace member cross section [mm],

t_w, t_f, t_1 – H/I-profile web and flange thickness and thickness of hollow section [mm],

r – radius of root fillet of the H/I-profile [mm],

θ_1 – the angle between connected bars [°],

γ_{M5} – partial factor for material properties [1,0]

$$b_w = \frac{h_1}{\sin\theta_1} + 5 \cdot (t_f + r) \le 2 \cdot t_1 + 10 \cdot (t_f + r) \tag{2}$$

2. Chord shear failure

$$N_{1,Rd} = \frac{f_{y0} \cdot A_v}{\sqrt{3} \cdot \sin\theta_1} / \gamma_{M5} \tag{3}$$

where:

A_0 – bottom chord cross section area [mm^2],

b_0 – width of the bottom chord [mm],

g – gap between braces [mm],

$$A_v = A_0 - (2-\alpha) \cdot b_0 \cdot t_f + (t_w + 2 \cdot r) \cdot t_f \tag{4}$$

$$\alpha = \sqrt{\frac{1}{1 + \frac{4 \cdot g^2}{3 \cdot t_f^2}}} \tag{5}$$

3. Brace failure

$$N_{1,Rd} = 2 \cdot f_{y,1} \cdot t_1 \cdot p_{eff} / \gamma_{M5} \tag{6}$$

where:

f_{y1} – yield stress of the brace member material [MPa],

b_1 – width of the brace member [mm]

$$p_{eff} = t_w + 2 \cdot r + 7 \cdot t_f \cdot f_{y0} / f_{y1} \le b_1 + h_1 - 2 \cdot t_1 \tag{7}$$

4. Brace failure with stiffener

$$\boxed{N_{1,Rd} = 2 \cdot f_{y,1} \cdot t_1 \cdot (b_{eff} + b_{eff,s}) / \gamma_{M5}} \tag{8}$$

where:

t_s – thickness of the stiffener [mm],

a – effective thickness of the stiffener weld [mm],

$$b_{eff} = t_w + 2 \cdot r + 7 \cdot t_f \cdot f_{y0} / f_{y1} \le b_1 + h_1 - 2 \cdot t_1 \tag{9}$$

$$b_{eff,s} = t_s + 2 \cdot a + 7 \cdot t_f \cdot f_{y0} / f_{y1} \le b_1 + h_1 - 2 \cdot t_1 \tag{10}$$

3.2 Load bearing capacities according to failure modes

1. Failure of web plate – buckling of the plate

$$b_w = \frac{100}{\sin 25°} + 5 \cdot (9 + 15) \le 2 \cdot 4 + 10 \cdot (9 + 15)$$

$$b_w = 355mm \le 248mm \Rightarrow \text{decides } \underline{248mm}$$

$$N_{1,Rd} = \frac{355 \cdot 6 \cdot 248}{\sin 25°} / 1{,}0 = 1240 \cdot 10^3 \, N = \underline{\underline{1240kN}}$$

2. Chord shear failure

$$\alpha = \sqrt{\frac{1}{1 + \frac{4 \cdot 26^2}{3 \cdot 9^2}}} = \underline{0{,}287} \qquad A_v = 3877 - (2 - 0{,}287) \cdot 160 \cdot 9 + (6 + 2 \cdot 15) \cdot 9 = \underline{1734mm^2}$$

$$N_{1,Rd} = \frac{355 \cdot 1734}{\sqrt{3} \cdot \sin 25°} / 1{,}0 = 769{,}3 \cdot 10^3 \, N = \underline{\underline{769{,}3kN}}$$

3. Brace failure – first design setup (with one stiffener)

$$p_{eff} = 6 + 2 \cdot 15 + 7 \cdot 9 \cdot 355 / 355 \le 100 + 100 - 2 \cdot 4 \quad \Rightarrow \quad p_{eff} = \underline{99mm} \le 192 \, mm$$

$$N_{1,Rd} = 2 \cdot 355 \cdot 4 \cdot 99 / 1{,}0 = 281{,}2 \cdot 10^3 \, N = \underline{\underline{281{,}2kN}}$$

4. Brace failure with stiffener – second design setup (with two stiffeners)

$$b_{eff} = 6 + 2 \cdot 15 + 7 \cdot 9 \cdot 355 / 355 \le 100 + 100 - 2 \cdot 4 \quad \Rightarrow \quad b_{eff} = \underline{99mm} \le 192 \, mm$$

$$b_{eff,s} = 8 + 2 \cdot 4 + 7 \cdot 9 \cdot 355 / 355 \le 100 + 100 - 2 \cdot 4 \quad \Rightarrow \quad b_{eff,s} = \underline{79mm} \le 192 \, mm$$

$$N_{1,Rd} = 2 \cdot 355 \cdot 4 \cdot (99 + 79) / 1{,}0 = 505{,}5 \cdot 10^3 \, N = \underline{\underline{505{,}5kN}}$$

According to resulting load bearing capacities, the decisive failure mode for the both design setups should be the *brace failure*. However, when the stiffener under the tension diagonal was considered, the load bearing capacity was nearly 80% higher than that reached for the setup without that stiffener. Numerical models then should show, if this expected behaviour would be confirmed, despite the fact that the aforementioned geometric condition was not fulfilled.

4 CHARACTERISTICS OF NUMERICAL MODELS

The models of the joint were created in the FEM software ANSYS 12.0 using the finite-elements, enabling both plastic behavior of materials and influence of large deformations. For modeling the HEA profile, 3D SOLID 65 finite element was used, defined by eight nodes and isotropic material properties. RHS bars were then modeled using shell finite element SHELL 43, defined by four nodes, four thickness values and orthotropic material properties [4].

The following material properties were used for the finite elements (cf., e.g. [5]): Young's module of elasticity E = 210 GPa, and Poisson's ratio ν = 0.3. Both physical and geometric non-linear aspects were considered within the calculation (a plastic calculation with regard to large deformations). The elasto-plastic behavior of materials was expressed by a bilinear diagram (cf., e.g., [6]) with yield stress f_y = 355 MPa and 5% hardening (it means that the value of the module of hardening is E_2 = 10 GPa).

The forces acting on the joint were chosen on the base of results obtained from a simple bar model of the entire girder (Fig. 3.) in such a way to preserve their ratio.

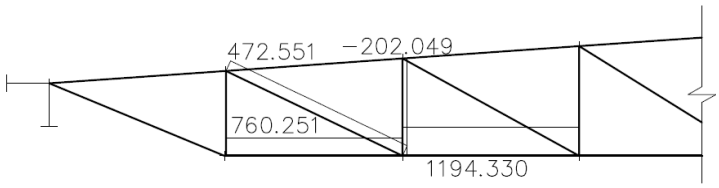

Fig. 3: Normal forces at the point of solved joint

On the basis of information available in the literature (e.g., [7], [8]), following boundary conditions were originally set (Fig. 4(a)):

- displacements in directions of the *x*, *y*, and *z* axes were prevented on both ends of the bottom chord, and the web braces were prevented from displacements both within the plane and out of the plane (hence displacements along the bar axes were only allowed).

However, such boundary conditions resulted in distribution of forces that did not correspond to the assumptions implied by the bar model. That is why we were looking for boundary conditions that would better correspond to the actual behavior of the selected detail of the lattice structure. Finally, the following boundary conditions were identified (Fig. 4(b)):

- only displacements in directions of the *x* and *z* axes (i.e., movements in the chord axis and out of its plane) were prevented, or the pin on the left end was replaced with a tensile-force load. The support preventing vertical displacement (in the direction of the *y* axis) was placed on the vertical brace.

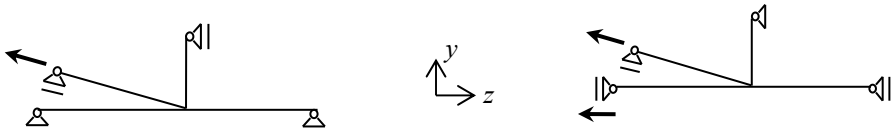

Fig. 4: (a) Original boundary conditions; (b) New boundary conditions.

Another possible solution of the problem of identifying suitable boundary conditions in the model is given by interconnecting the structure's 3D detail with the 2D bar members and modeling the lattice structure as a whole (cf. Fig. 5.). The boundary conditions and load would then be related to the entire structure and detail's behavior would be derived from the entire structure's behavior. Correctness of this hypothesis and implementation of such a model must, however, be subsequently verified.

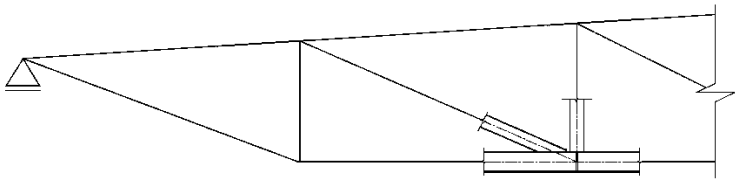

Fig. 5: Connection between the bar and 3D models

5 EVALUATION OF THE RESULTS

Following four models were studied:

- a joint with a stiffener under the compression vertical brace only, loaded with a tensile force in the diagonal brace,
- a joint with a stiffener under the compression vertical brace only, loaded with a tensile force in both the diagonal brace and the bottom chord,
- a joint with a stiffener under both the compression vertical brace and the tension diagonal brace, loaded with a tensile force in the diagonal brace and
- a joint with a stiffener under both the compression vertical brace and the tension diagonal brace, loaded with a tensile force in both the diagonal brace and the bottom chord.

Apart from the evolution of stresses, we also investigated dependency of the HEA profile flange plate central part's (point 2) vertical deformation (uy) on that of the HEA profile flange plate edge part's (point 1) deformation values (Fig. 6. and 7.), namely, at two sections: under the edge of the connected diagonal brace (section A) and near the center of this brace (i.e., near the connection point of the second stiffener - section B) – cf. Fig. 8. – 10.

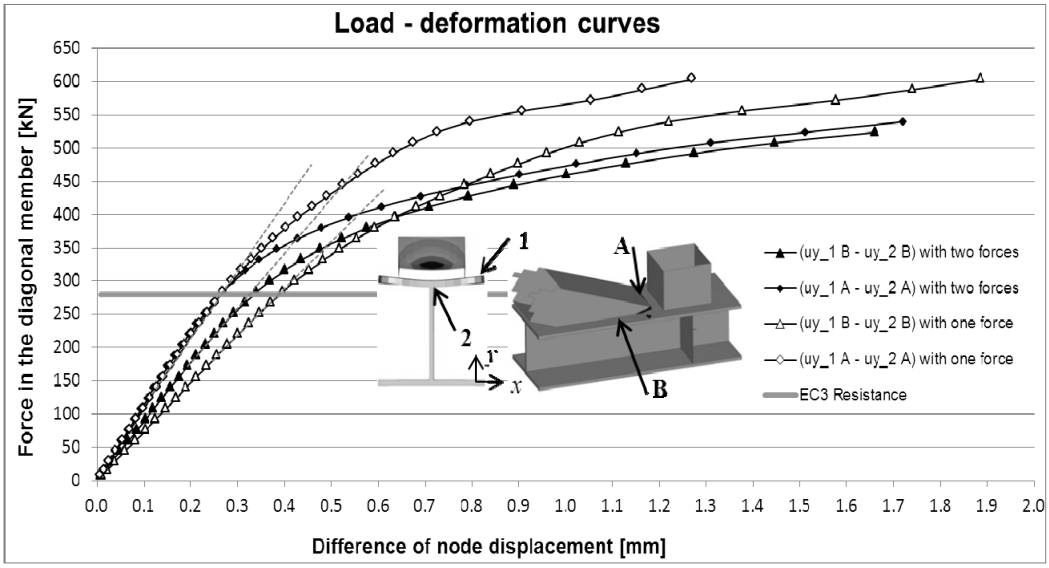

Fig. 6: Load-deformation curves for single-stiffener models
and the comparison with the Resistance according to EC3.

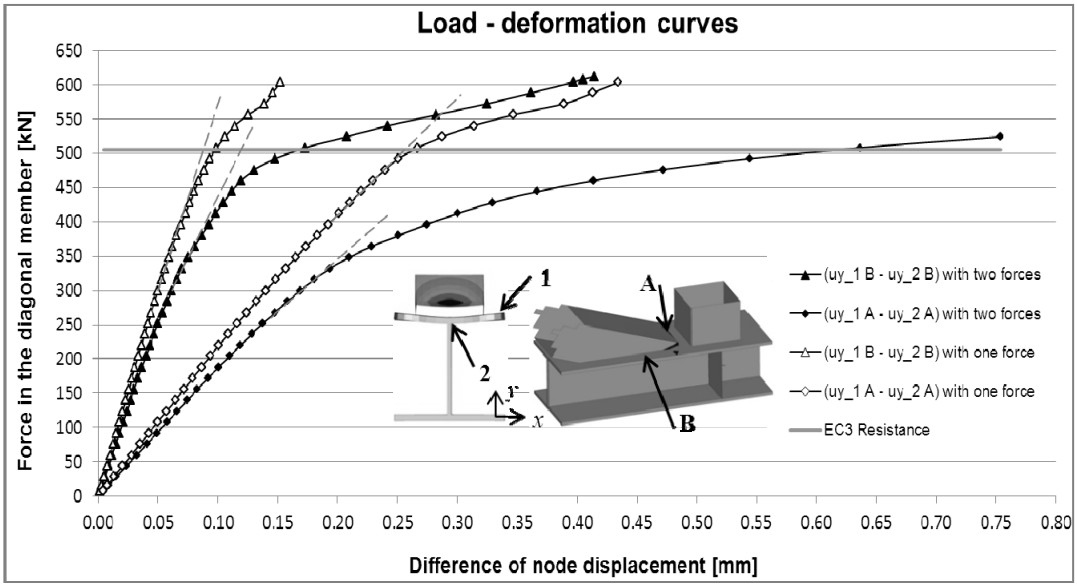

Fig. 7: Load-deformation curves for double-stiffener models
and the comparison with the Resistance according to EC3

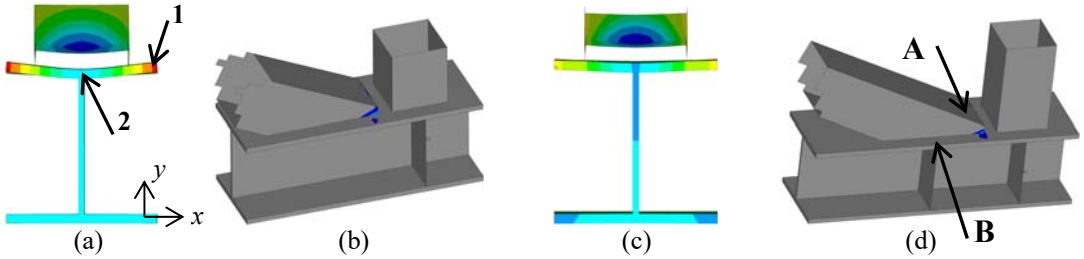

Fig. 8: Comparing the flange plate deformation values and plastic stress evolution of unstiffened (a)+(b) and stiffened (c)+(d) HEA profile when loaded with a force of **300 kN** in the diagonal brace (the deformation values are 20× magnified).

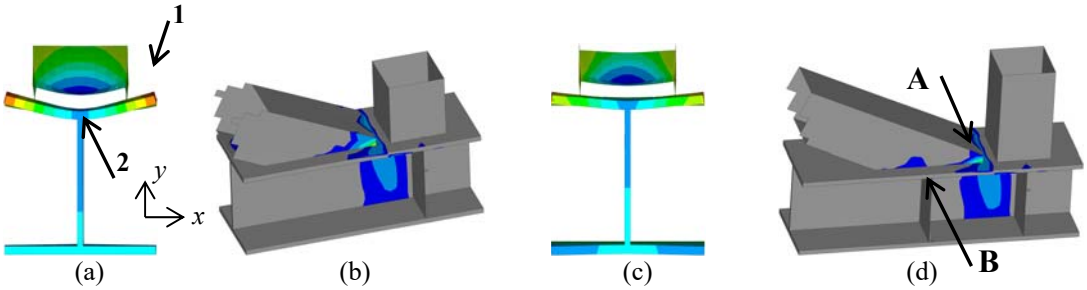

Fig. 9: Comparing the flange plate deformation values and plastic stress evolution of unstiffened (a)+(b) and stiffened (c)+(d) HEA profile when loaded with a force of **444 kN** in the diagonal brace (the deformation values are 20× magnified).

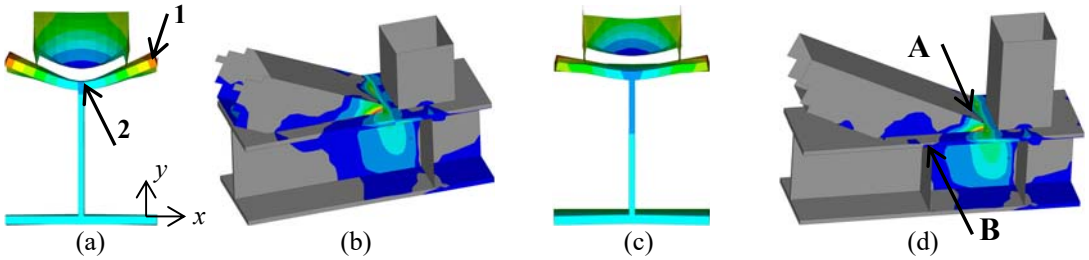

Fig. 10: Comparing the flange plate deformation values and plastic stress evolution of unstiffened (a)+(b) and stiffened (c)+(d) HEA profile when loaded with a force of **508 kN** in the diagonal brace (the deformation values are 20× magnified).

6 CONCLUSION

A numerical model was created which fits the expected behaviour of the joint. One of the conclusions of this paper is that the load-bearing capacity of the joint is not significantly influenced by loading the tension brace only, or both the tension brace and the bottom chord. The only significant difference is given by total deformation values, which confirms the principle of calculating load-bearing capacity of such a joint according to EC3.

Seeing the load-deformation curves presented at Fig. 6. and 7. it can be concluded that the joint with stiffener under the diagonal brace was able to carry significantly higher load than the joint without that stiffener. Taking into account increase of the difference between deformation of central and edge part of the HEA-profile top flange, the load bearing capacity for particular design setup can be determine. The capacity of the joint with one stiffener will be around 300 kN and the double stiffened joint will be able to carry more than 508 kN. The first type of models (one stiffener) obviously showed signs of *brace failure*, while for the second type of models (two stiffeners) this type of failure was not so clear. Considering the evolution of the plastic stresses and the deformation of the whole joint in the second design setup, the failure mode could be classified rather as a *chord shear failure*. The problem of determination the decisive type of failure for numerical model requires further and more detailed modelling and researching.

Besides the already mentioned, the results obtained by investigation of the deformations of HEA-profile flange pairs of point showed, that even if the joint geometry goes beyond the Eurocode limitations, behaviour and load-bearing capacity of this joint are very close to the expectations implied by that standard.

ACKNOWLEDGMENTS

This research was financially supported by Project MŠMT number SP2012/135.

REFERENCES

[1] ČSN EN 1993-1-8, Eurocode 3: Design of steel structures - Part 1-8: Design of joints. Český normalizační institut, 2006. 126 pp.

[2] Wald, F., Sokol, Z. *Navrhování styčníků*. Praha: Vydavatelství ČVUT, 1999. 144 pp. ISBN 80-01-02073-8. (in Czech)

[3] Wardenier, J. *Hollow Sections in Structural Applications*. CIDECT, 2001. ISBN 0-471-49912-9

[4] *Release 11.0 Documentation for ANSYS* [online]. [cit. 2012-4-25]. Available from <http://www.kxcad.net/ansys/ANSYS/ansyshelp>

[5] Jurčíková, A., Rosmanit, M.: Numerické modelování svařovaného T-styčníku. *Sborník vědeckých prací Vysoké školy báňské - Technické univerzity Ostrava, řada stavební,* Ostrava. Číslo 2, 2011. Ročník XI. ISSN 1213-1962, 6 pp. (in Czech)

[6] de Lima, L. R. O., Vellasco, P. C. G. da S., da Silva, J. G. S., Neves, L. F. da C., Bittencourt, M. C. A numerical analysis of tubular joints under static loading. In *Proceedings of APCOM'07 in conjunction with EPMESC XI*, Kyoto, Japan. December 3-6, 2007.

[7] Vegte, G. J. van der, Makino, Y., Wardenier, J. The influence of boundary conditions on the chord load effect for CHS gap K-joints. In *Connections in Steel Structures*. Amsterdam. June 3-4, 2004.

[8] Choo, Y. S., Qian, X. D., Wardenier, J. Effects of boundary conditions and chord stresses on static strength of thick-walled CHS joints. In *Journal of Constructional Steel Research*., Volume 62, Issue 4, April 2006, Pages 316–328

Reviewers:

Prof. Ing. Stanislav Kmeť, PhD., Department of Steel and Timber Structures, Faculty of Civil Engineering, Technical University of Košice.

Ing. Milan Pilgr, Ph.D., Institute of Metal and Timber Structures, Faculty of Civil Engineering, Brno University of Technology.